Modeling of RF Head Exposure in Children

J. Wiart,[1]* A. Hadjem,[1] N. Gadi,[1,2] I. Bloch,[2] M.F. Wong,[1] A. Pradier,[1] D. Lautru,[3] V.F. Hanna,[3] and C. Dale[1]

[1]R&D of France Telecom, Moulineaux, France
[2]Ecole Nationale Supérieure des Télécommunications, Moulineaux, France
[3]University of Paris VI, France

This study analyzes the main parameters that should influence the specific absorption rate (SAR) in children's heads. The evolution of their head shape and the growth of specific parameters, such as the skull thickness, are analyzed. The influence of these parameters on the radio frequency (RF) exposure of children's head is studied. The SAR over 1 g in specific tissue is assessed in different children's head models based on magnetic resonance imaging (MRI) and on non-uniformly down-scaled adult heads. Comparisons with SAR data in adults are reported using a handset with a patch antenna operating at 900 MHz. Bioelectromagnetics Supplement 7, 2005. © 2005 Wiley-Liss, Inc.

Key words: radiofrequency; specific absorption rate; mobile telephone; handset; FDTD

INTRODUCTION

With the increasing number of children using mobile phones, there is concern about their exposure to radio frequency (RF) fields and their possible sensitivity to RF. Even though international bodies, such as the International Commission on Non-Ionizing Radiation Protection (ICNIRP) or the Institute of Electrical and Electronic Engineers (IEEE), have developed exposure limits to protect the general public against overexposure to electromagnetic fields [ICNIRP, 1998; IEEE, 1999], the public concern still exists.

From an exposure assessment point of view, the questions are, on the one hand about the comparisons of power absorbed by children heads to those absorbed by adults, and on the other hand about the validity for children of specific absorption rate (SAR) compliance testing methods that are now required to check compliance with the limits defined by international bodies such as ICNIRP.

Previous studies based on numerical methods have been carried out to analyze the energy absorption of RF fields from handsets in the heads of children [Gandhi et al., 1996; Schoenborn et al., 1998; Gandhi and Kang, 2002; Wang and Fujiwara, 2003]. This energy deposition has been compared to the absorption observed in adults. Because a variety of head models and RF sources have been used, comparisons are often difficult. For instance, children's heads have been modeled using uniform or non-uniform scaling of adult models, or using magnetic resonance imaging (MRI) data to build an appropriate model. Besides the choice of head model, the position of the handset relative to the head and the modeling of the handset also have a large influence on the SAR induced in tissues, further complicating any comparison between the different studies.

This study analyzes the main parameters that should influence the SAR in children heads. We study the evolution of the head shape and the growth of specific parameters, such as the skull thickness. The SAR over 1 g in specific tissues is assessed for different types of children head models based on non-uniformly down-scaled adult heads as well as on MRI data. Comparisons with SAR in adults are performed.

MATERIALS AND METHODS

SAR Assessment Using Numerical Method

Specific absorption rate estimation. The SAR in a given tissue is given by the well known relationship $\sigma E^2/2\rho$ where σ is the conductivity of the tissue, E the electric field strength in tissue, and ρ the mass density.

Grant sponsor: RNRT network (Réseau National de Recherche en Télécommunication).

*Correspondence to: J. Wiart, France Telecom RD, RESA FACE IOP, 38-40 Rue du General Leclerc, 92794 Issy les Moulineaux, France. E-mail: Joe.wiart@rd.francetelecom.com

Received for review 14 October 2004; Final revision received 2 May 2005

DOI 10.1002/bem.20155
Published online in Wiley InterScience
(www.interscience.wiley.com).

© 2005 Wiley-Liss, Inc.

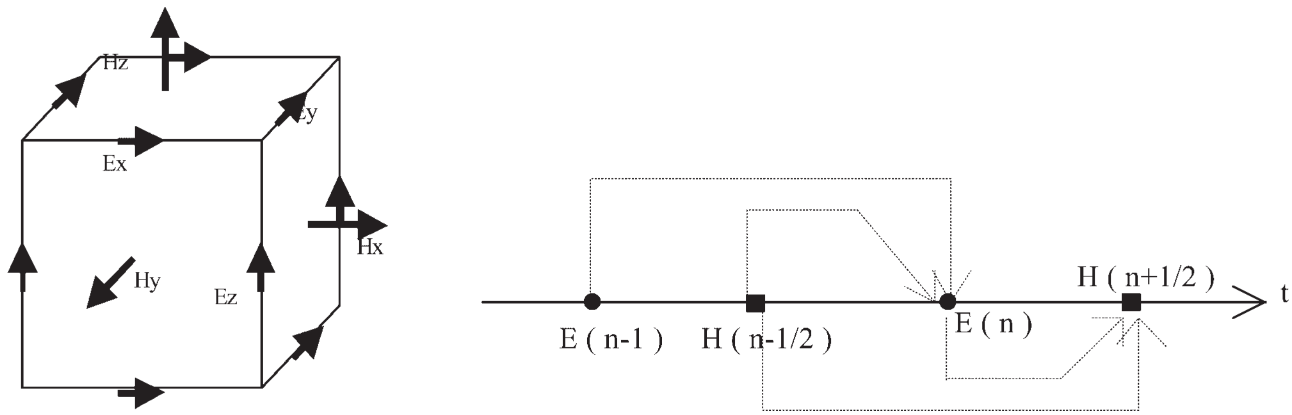

Fig. 1. Yee cell and the "leap frog" scheme of the FDTD method.

Different numerical methods can be used to assess the electric field and the human exposure to RF emissions. The aim of this section is not to review all the methods but rather to give the reader an outline of the popular finite difference time domain (FDTD) method.

The FDTD has been intensively studied and has proved its intrinsic accuracy and its ability to estimate the SAR in heterogeneous media [Taflove, 1995]. In the FDTD procedure, Maxwell's equations are discretised in both space and time using central difference formulas of second-order accuracy (with uniform grid), on a staggered Yee-grid, as shown in Figure 1 for the 3D case, where *E* and *H* are respectively the electric and magnetic fields. This gives rise to the well-known temporal ''leap frog'' scheme in one dimension. In 3D, vectors components are involved [Taflove, 1995] but the principle is the same.

Because of memory limitations the computational domain has to be a finite volume and absorbing boundary conditions have to be imposed on the borders of the domain. The perfectly-matched layer (PML) [Berenger, 1994], which results in very low spurious reflections, is an absorbing boundary condition that is nowadays intensively used in FDTD SAR calculations.

SAR in heterogeneous adult head models. The SAR estimation of a heterogeneous head requires an accurate volumetric model of the head. Nowadays the most popular model of this type is the ''Visible Human'' (http://www.nlm.nih.gov/research/visible/visible_human.html), whose segmentation was performed by Brook's Air Force Base in the United States.

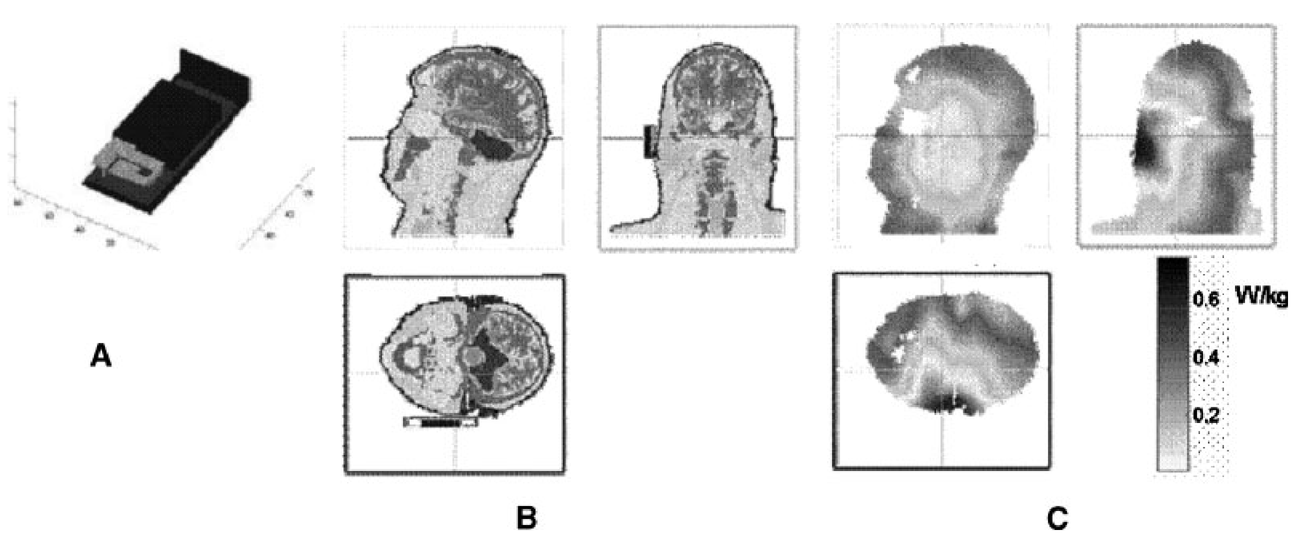

Fig. 2. **A**: Handset model with a patch antenna, (**B**) head model, and (**C**) computed SAR (W/kg) in head tissues.

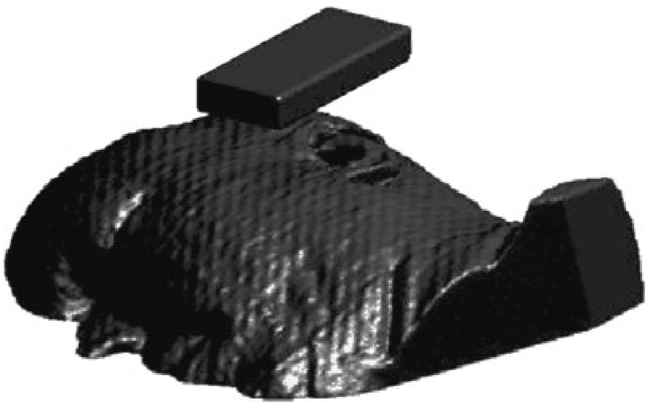

Fig. 3. Profile of the skin surface close to the mobile.

Using this adult head model, the SAR can be numerically estimated for any handset model by applying the FDTD computational method (Fig. 2).

The accuracy of the numerical RF exposure assessment does not only depend on the numerical method used which in this case is very good, and on the accuracy and representativeness of the head model, but also on the positioning of the mobile phone relative to the head (Fig. 3).

The presence of the head has an influence on the antenna impedance of the handset. To compare simulations, one can consider either of two scenarios: the current delivered by the amplifier to the antenna is constant (in this case the emitted power is varying) or the power delivered by the amplifier is constant. A previous study that analyzed this question [Wang and Fujiwara, 2003] showed that this is a possible source of uncertainty. In our simulations, we have considered a constant power emitted (i.e., independent of the head) which seems to be a realistic assumption in the RF domain.

SAR calculations were performed on three different head models derived from MRI data. Besides the visible human mentioned above (shown in Fig. 11), two other French models were used, namely the FTRD adult head (shown in Fig. 7) and the COMOBIO head model. Using a handset with a patch antenna (as in Fig. 2), the maximum SAR over 10 g was calculated and compared at 900 and 1800 MHz, showing large differences between the head models. At 1800 MHz the maximum SAR over 10 g varies from 0.14 to 0.49 W/kg with a mean value of 0.34 W/kg, and at 900 MHz the values vary from 0.61 to 1.24 W/kg with a mean value of 0.85 W/kg.

The results beg the question of how representative any of these head models are, and in particular of the choice of the visible human model as a reference. Based

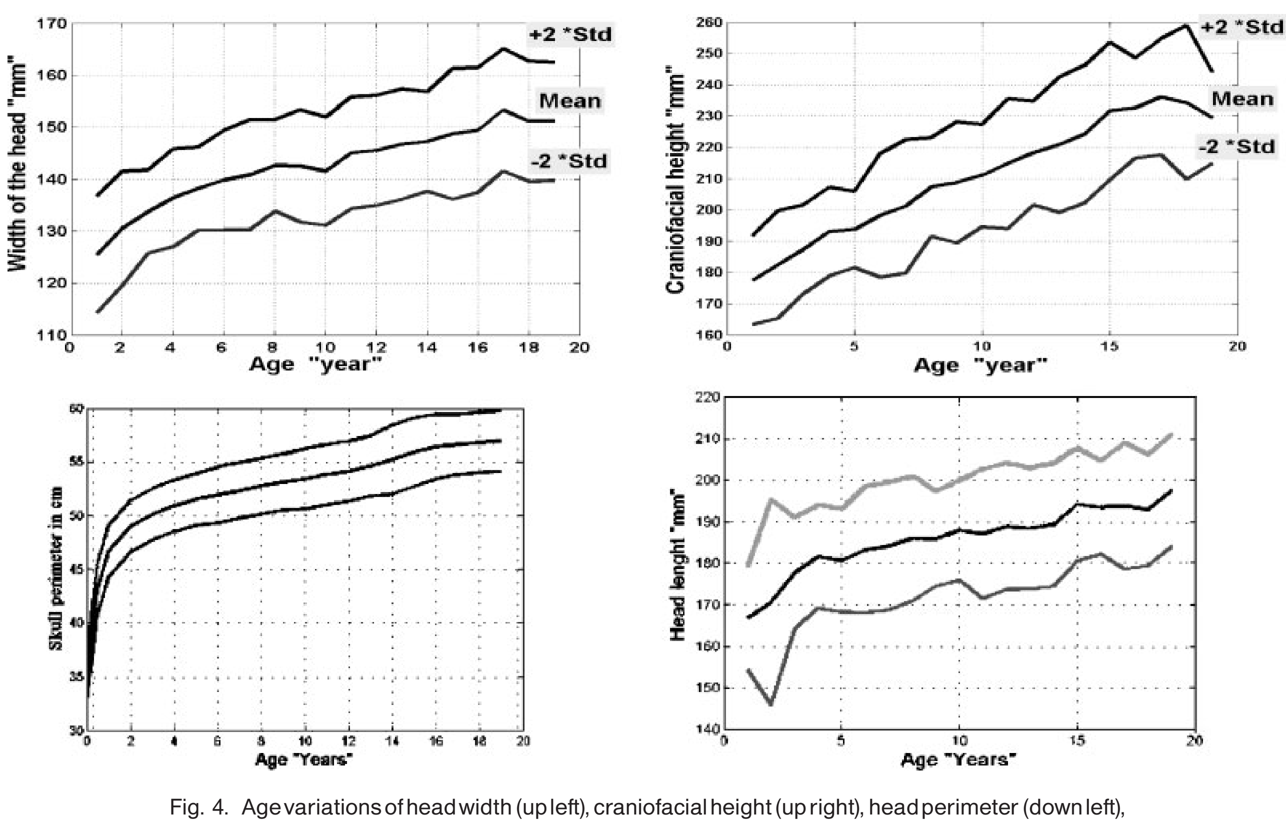

Fig. 4. Age variations of head width (up left), craniofacial height (up right), head perimeter (down left), and head length (down right).

Fig. 5. Different proportions between adult head (left) and child head (right).

on the observed differences between SAR induced in different adult head models, the variability of the SAR over 10 g can be estimated at least ±30%. Any comparison of SAR assessed in a child's head will prompt the same question.

Child Head Model

To analyze the SAR in children's heads, representative models have to be defined. The anthropometry of their head and face as well as the morphology of their body are age dependent [Sempé, 1979; Farkas, 1994]. The variations of parameters, such as head perimeter, craniofacial height (i.e., head height), head length (head size in the direction orthogonal to the face), and width as a function of age are given in Figure 4, where it can be observed that these parameters do not grow uniformly.

An important feature to note is that the proportions of an adult head and a child head are different (Fig. 5). The first models of children's heads used in the literature to assess RF exposure were based on uniform downscaling of an adult head [Gandhi et al., 1996], where the head of a child was considered as a small adult head. However, this approach does not take into account for the fact that the proportion of the head is age dependent. For instance, if an adult head size is downscaled uniformly to 85% of its original size to correspond to the outer dimensions of child, then the brain volume is equivalent to the one of a newborn child. Because of this shortcoming, the uniform downscaling does not provide an accurate child head representation.

Other approaches, such as the "Child-Like" model, have been developed using a method based on non-uniform downscaling of an adult head [Wang and Fujiwara, 2003]. The child-like head is built by morphing deformation of an adult head. In this case, the adult head is divided in different parts (Fig. 6) and specific downscaling is applied to each of these parts. The method allows creating age-specific head model such as those shown in Figure 7.

The main limit of this approach is linked to the non-uniform growth of organs. The head, the volume of the brain, the skin, and skull thickness [Koenig et al.,

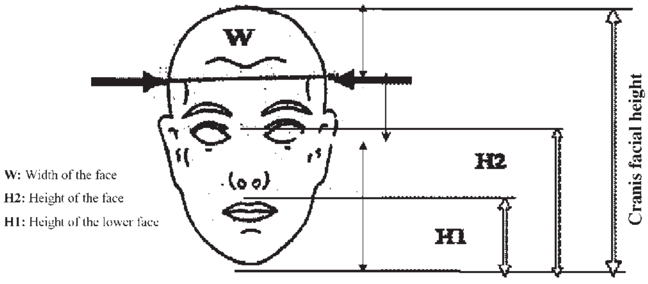

Fig. 6. Morphing principle: Head divided in different parts.

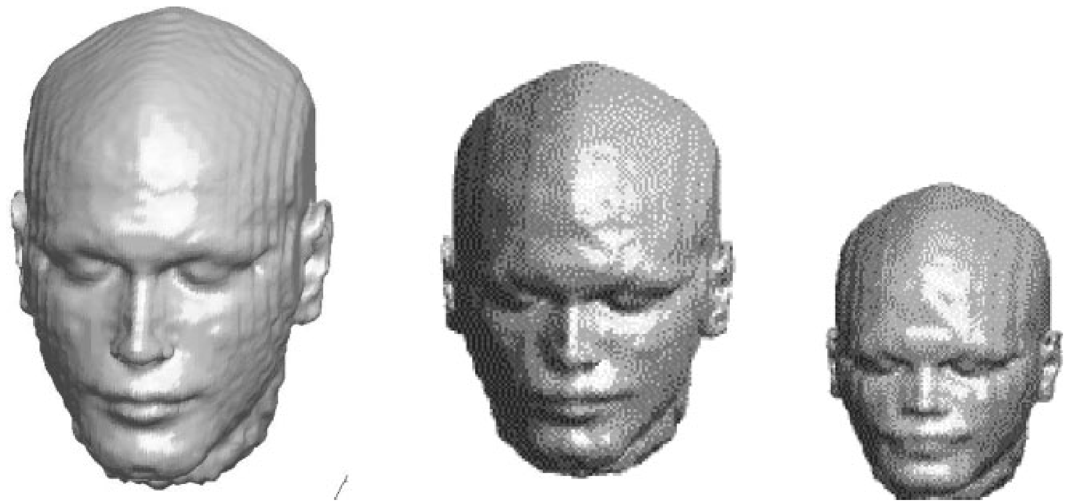

Fig. 7. Adult head model developed by FTRD (left), 12 year old child-like head (center), and 4 year old child-like head (right).

1995; Seidenari, 2000] each grow at different rates. Figure 8 shows the age variation of the temporal skull thickness and the brain mass. The neurocranium of a 1-year-old child has a volume of 900 cm^3, about 1200 cm^3 for a 5 years old and the volume of an adult skull is about 1300–1450 cm^3. From 5 to 18 years, the volume of the brain is quite constant while the thickness of the skull increases by about 75%.

The thickness of the skin also varies with age [Seidenari, 2000]. As shown in Figure 9, the forehead skin thickness is 1.18 ± 0.22 at 2–3 years, 1.56 ± 0.36 at 11–13 years, and 1.99 ± 0.34 for adults.

Because of such different growth patterns for different parts of the head, the SAR analysis is best done using children head models based on MRI data. The French ADONIS program (www.tsi.enst.fr/ADONIS) of the RNRT research network (www.telecom.gouv.fr/rnrt) is working to build age-dependent children head models (Fig. 10) with eight tissues and a millimetric resolution using MRI data.

While defining child head models based on MRI is important, there is also a notable variability within an age group. For instance, as shown in Table 1, the characteristics of the 12 year old child of Figure 10 are within 95% of the related class, nevertheless the height is like a 10 year old mean child, the width is like a 15 year old mean child.

The electromagnetic properties of tissues are needed to estimate the SAR locally. In this study, we employ those internationally used [Gabriel, 1996]. In this study, we focus the SAR analysis on the influence of morphology and neglect the age variation of dielectric properties [Van Rongen, 2004].

CHILD HEAD EXPOSURE: ANALYSIS OF RF ABSORPTION

International bodies such as IEEE, IEC, and CENELEC have developed methods [IEEE, 1999; CENELEC EN50361, 2001; IEC PT 62209 Part 1, 2005] to test the compliance of handset products to related limits. A homogeneous phantom, the specific anthropomorphic mannequin (SAM), has been defined with a shape and equivalent liquid that provide a conservative approach (i.e., the SAR assessed in SAM is always above the SAR induced in a real heterogeneous head) of the measured SAR over 10 g. These international standards also define testing positions, namely cheek and tilted. Since SAM is based on studies carried out on adult heads [Drossos et al., 2000], it is of interest to check if this approach is also conservative for children. To that end, RF absorption calculations were carried out using different children head models and compared to data for adults.

"Child-Like" Models Based on Morphing

Comparison with SAM. SAR calculations were performed on SAM and the child-like model, employing the same phone models (Fig. 11) as those used in an ongoing international inter-comparison coordinated by the US food et drug administration (FDA) [Beard, 2003]. The normalized maximum SAR over 10 g of tissue is shown in Figure 12 for both models at 835 and 1900 MHz. In all these cases, the SAR over a mass of 10 g has been assessed in all tissues involved (i.e., including pinna tissues). The SAR is estimated in SAM

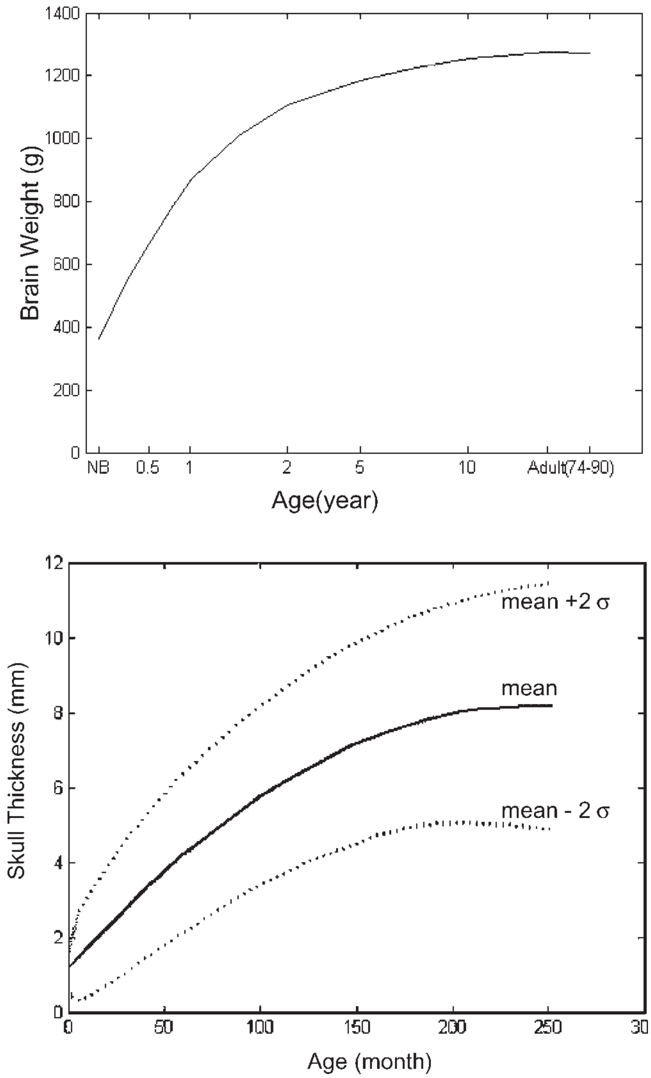

Fig. 8. Related age variation of the temporal skull thickness (right) and the brain mass (left) [after Koenig et al.,1995].

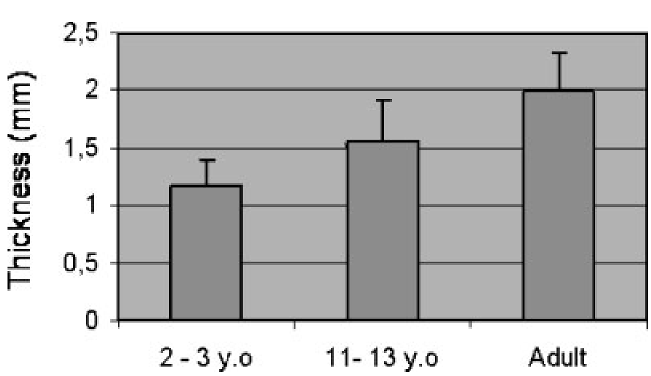

Fig. 9. Thickness of the forehead skin (mm) versus age.

to be more than twice the value in the child head and so SAM is conservative for the child-like head considered.

As discussed in the introduction, the question is not only to estimate the validity of compliance testing method but also to analyze the specificity of children absorption and to compare this distribution to the adult one. To achieve this objective a specific analysis of children has to be done.

Analysis of age dependence. First, a comparative analysis of the RF absorption in different tissues within the head (skin, muscle, skull, CSF, and brain) is performed as a function of age (4 years old, 12 years old, and adult). Technical variables include the frequency of operation (900 and 1800 MHz) and the type of handset. Three handsets are compared, that is, one with a patch antenna, one with a dipole lined up with ear and mouth located at 7 mm distance from the pinna and parallel to a cheek position, and the handset used in the IEEE/FDA study (Fig. 11) in cheek position. In each case, the power emitted by the phone is considered as constant (i.e., independent of the head). The advantage of the dipole is to minimize the uncertainty due to the positioning of the phone (since it does not touch the skin, the positioning uncertainty is smaller).

Using child-like models (Fig. 7) and different handset models, the maximum SAR over 1 g of different tissues has been estimated in the cheek position at different frequencies. As can be seen in Figure 13, the ratio between SAR in the adult and the child-like heads depends both on frequency and handset type.

The mean value of the ratio (maximum SAR over 10 g in the child head) over (maximum SAR over 10 g in the adult head) is 0.92 at 900 MHz and 0.83 at 1800 MHz with standard deviation of 0.17 and 0.12, respectively. Over 1 g, these ratios are 0.98 at 900 MHz and 0.91 at 1800 MHz with standard deviation of 0.21 and 0.20, respectively. The differences between the maximum SAR over 10 g estimated in the adult head and in the child-like heads are less than 25% (Fig. 14).

The SAR in child-like brain tissues is larger than in adult brain (ratio above 1 in Figure 14). Since the morphing has reduced the thickness of the skull and skin down to 10%, it is quite logic to have as shown in Figure 14 a higher SAR in the brain of children compared to the SAR in the brain of an adult. However in both cases as shown in Figure 13, the SAR in the brain is very small compared to the SAR in skin and muscle.

The morphing is based on the external shape of the head. We analyzed the validity of this approach using a patch antenna. The maximum SAR over 10 g in a 12 year old visible human head and a 12 year old MRI head are compared: the model based on the visible human has

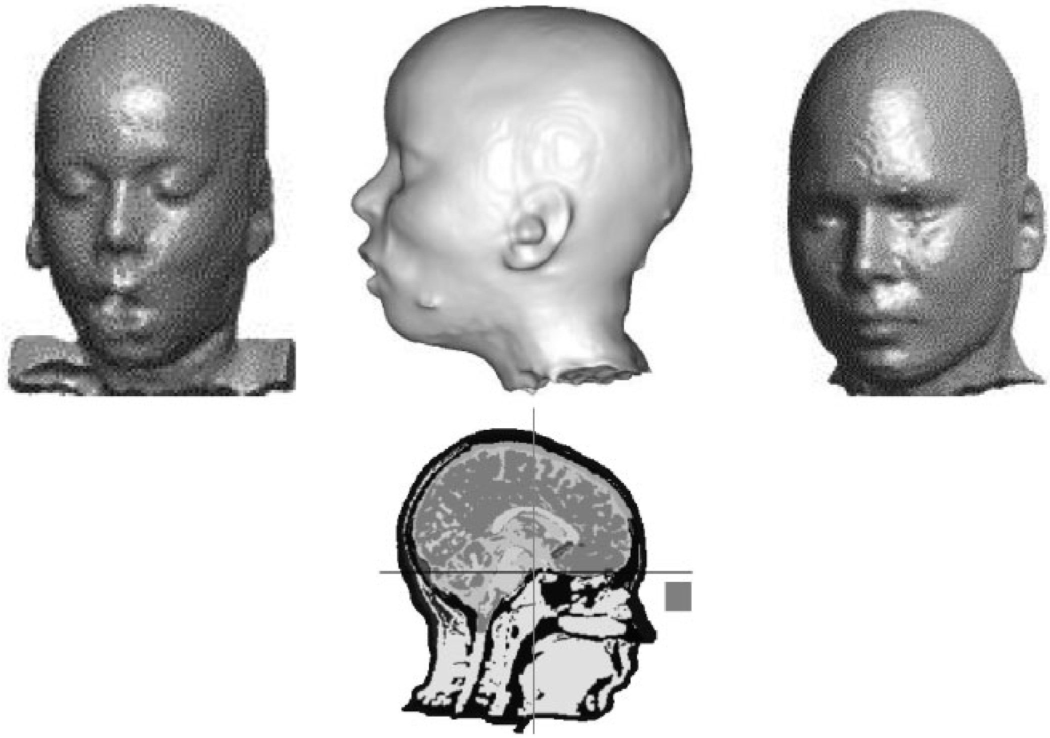

Fig. 10. From left to right: Children head models of a 4 year old, 5 year old, 12 year old, and sagittal view of the 12 year old (below).

TABLE 1. Characteristics of Children Head Models Developed Under the Umbrella of the ADONIS Project

Age	Height in cm	Δ/mean (in σ)[a]	Equiv. age in years	Width in cm	Δ/mean (in σ)	Equiv. age in years
4 years old	18.5	−0.6	3	18.5	+0.5	8
12 years old	21	−1	10	19.5	+0.9	15

[a]σ is the standard deviation.

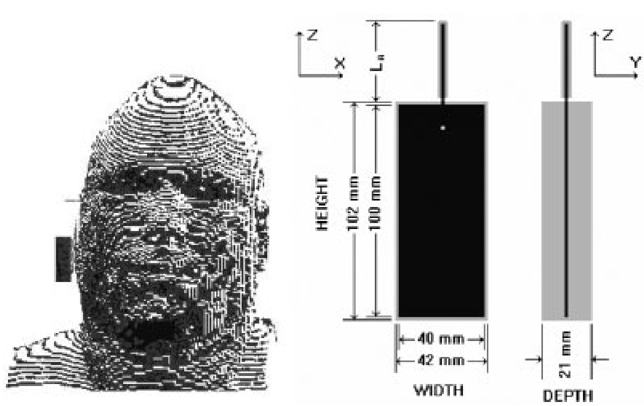

Fig. 11. Visible Human and the "IEEE" handset.

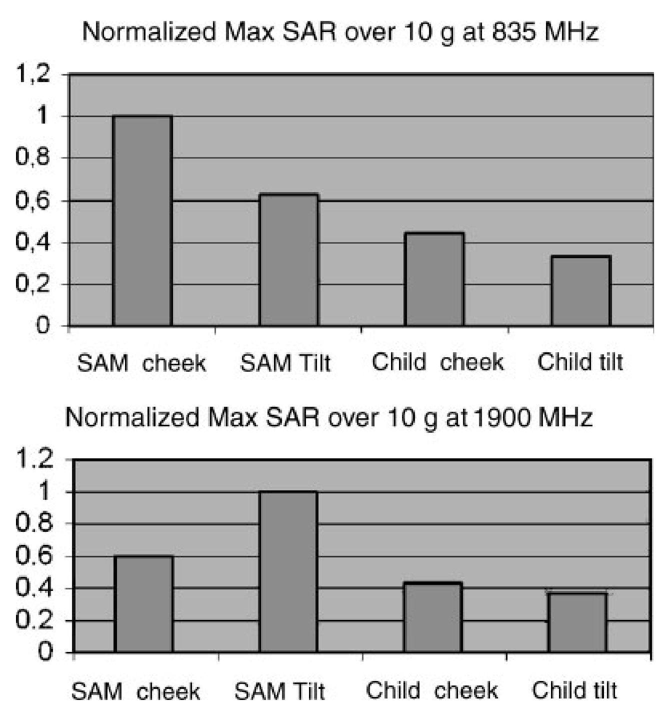

Fig. 12. Normalized maximum SAR over 10 g of tissues (**a**) 835 MHz, (**b**) 1,900 MHz.

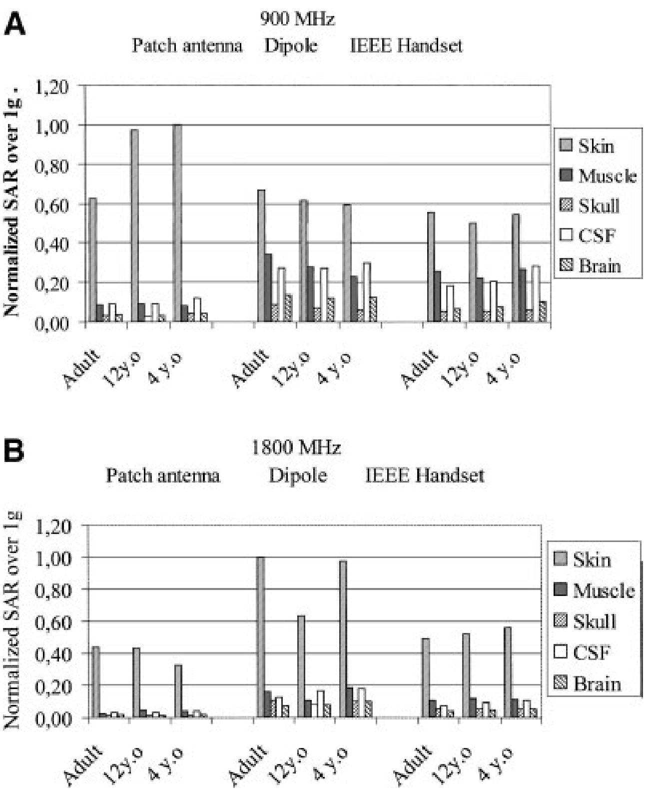

Fig. 13. **A**: Normalized (to 250 mW) SAR over 1 g induced in different tissues of adult and child like heads versus handset at 900 MHz. **B**: Normalized (to 125 mW) SAR over 1 g induced in different tissues of adult and child-like heads versus handset at 1,800 MHz.

a maximum SAR over 10 g 30% higher than the one based on MRI.

The SAR induced in different tissues has also been assessed. As shown in Figure 15, the SAR over 1 g in the skin of a 12 year old based on visible human is overestimated but the SAR over 1 g in brain of this latter is underestimated.

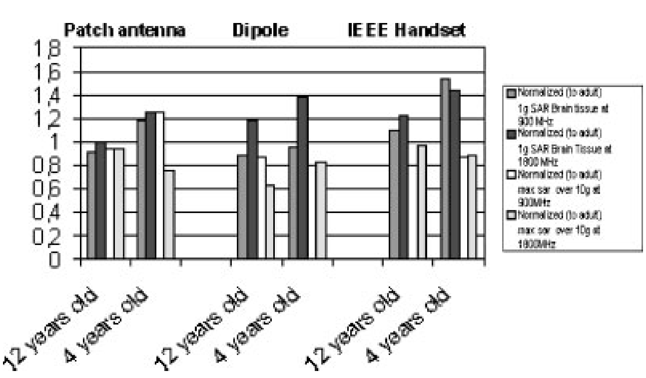

Fig. 14. Normalized max SAR over 1 g brain exposition and normalized max SAR over 10 g (all tissues) for adult and children for different frequency and handset.

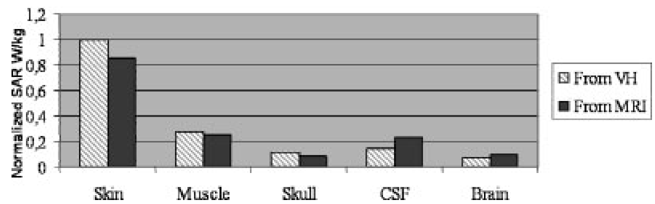

Fig. 15. Normalized SAR (to the max SAR over 1 g in the head skin derived from visible human) for different tissues in a 12 year old child head (child like derived from the visible human and model from MRI).

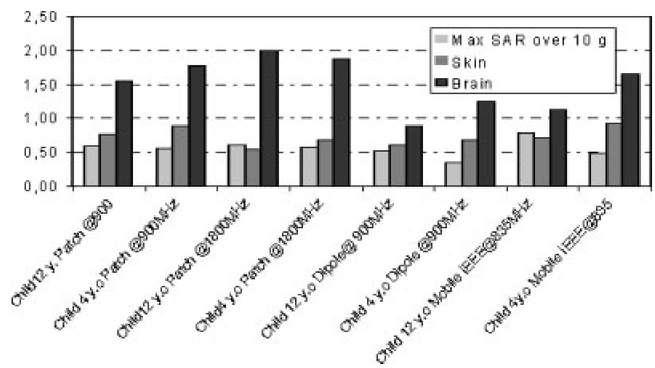

Fig. 16. Ratio of max SAR in tissues assessed in children MRI-based model relative to the FTRD adult model.

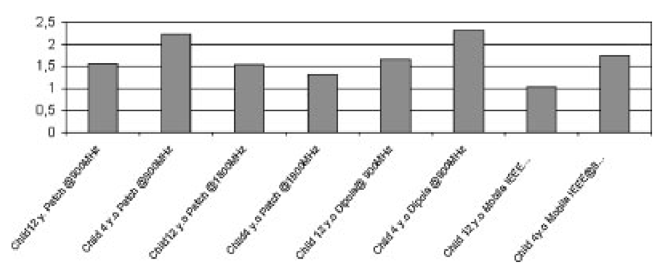

Fig. 17. Ratio of max SAR over 10 g assessed in child-like models and in MRI based.

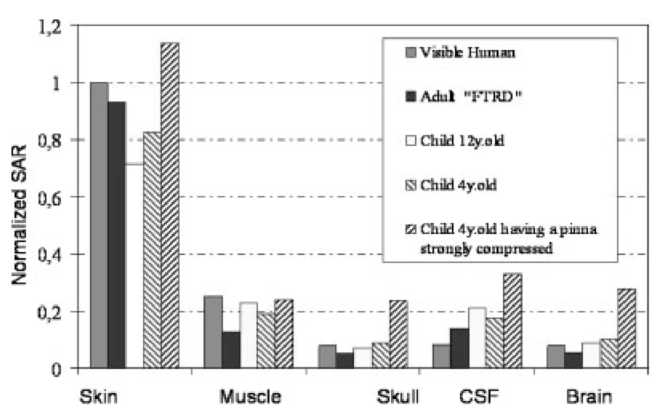

Fig. 18. SAR in head tissues (normalized to SAR over 1 g equal to 1 W/kg in the visible human skin) using a handset with patch antenna operating at 900 MHz in cheek position.

TABLE 2. Maximum SAR over 10 g Normalized to 1 W/kg in Visible Human

	Visible human	Adult "FTRD"	12 year old child	4 year old child	4 year old child having a pinna strongly compressed
Max SAR over 10 g	1 W/kg	1.7 W/kg	1 W/kg	0.9 W/kg	1.6 W/kg

Child Models Based on MRI Data

To perform MRI on young children (under 6 years) the head is usually wedged in order to limit possible movements. The pinna is therefore strongly compressed, which does not accurately represent the shape of the pinna of the child during a mobile phone conversation. Hence using unaltered MRI data would provide an overestimation of the SAR since the mobile phone would be modeled closer to the head. To circumvent this problem, the MRI model has been slightly modified to reduce the pressure on the pinna and to allow comparisons with the other head models.

We calculated the maximum SAR over 1 g of skin, muscle, skull, CSF, and brain using different phone models (patch, dipole, and a quarter wavelength on a box) and heads (adult, 12 years old and 4 years old) based on MRI data. Calculations were carried out at different frequencies (835, 900, and 1800 MHz). In all cases, the power emitted by the phone was considered constant (i.e., independent of the head). Moreover we observed that the real part of the impedance varied by less than 20%.

Results obtained from head models based on morphing (child-like) and on MRI data are compared in Figures 14, 15, 16, 17. The figure shows that child-like models used in this study overestimate the SAR over 10 g assessed in MRI-based head model. However, since head models generally have large variability, further analyses are required before firm conclusion.

The ratio between the max SAR over a given mass of tissues in children and adults is given in Figure 16. The extrapolation of such results is complex since on one hand, the position of the phone may also have a large influence on the SAR assessment, and on the other hand the question of the representativeness of child and adult heads used is still open.

We compared the SAR induced in specific tissues with different heads of adults and children using the handset having a patch antenna operating at 900 MHz in a cheek position (Fig. 18). The SAR over 10 g depends on the head model, as shown in Table 2 the SAR over 10 g calculated in Visible Human is, in this configuration, lower than the one estimated in the "FTRD" head. The Table 2 shows that the maximum SAR over 10 g assessed in child MRI-based head models is comparable to the SAR calculated in adult heads.

Moreover, as expected, the model having a strongly compressed pinna has a higher SAR in tissues than the model having a realistic compression. Figure 18 shows also that the SAR induced in the children brain is slightly higher than the adult ones. This being said, the level of exposure in the brain remains very low.

FETUS EXPOSURE

In the analysis of children exposure to RF, the fetus represents a specific situation. Assessing the exposure of the fetus is difficult since MRI procedures are

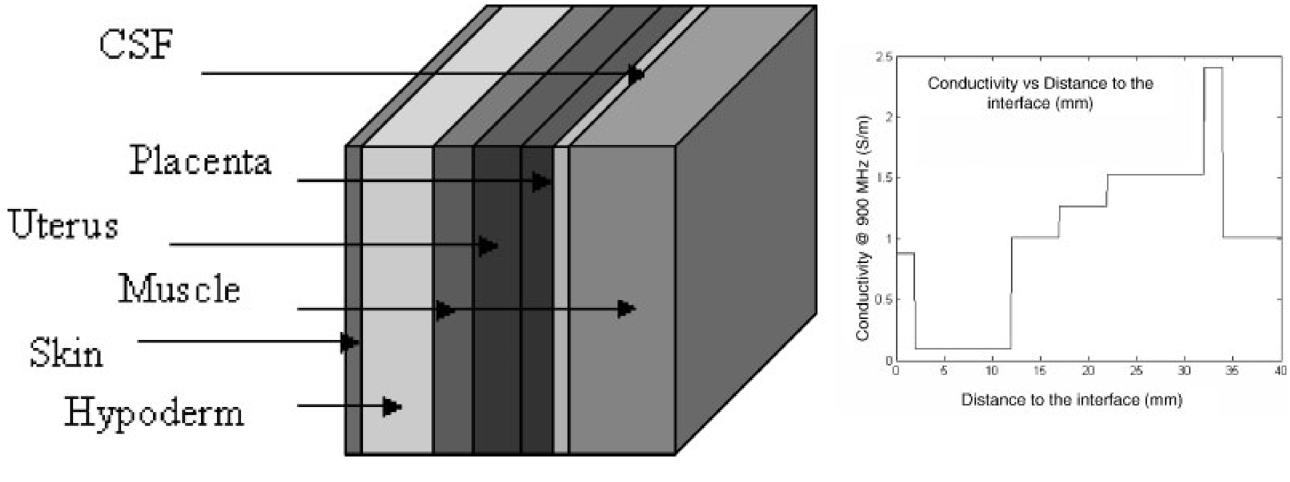

Fig. 19. Planar multiplayer structure (left) and conductivity of the various layers at 900 MHz (right).

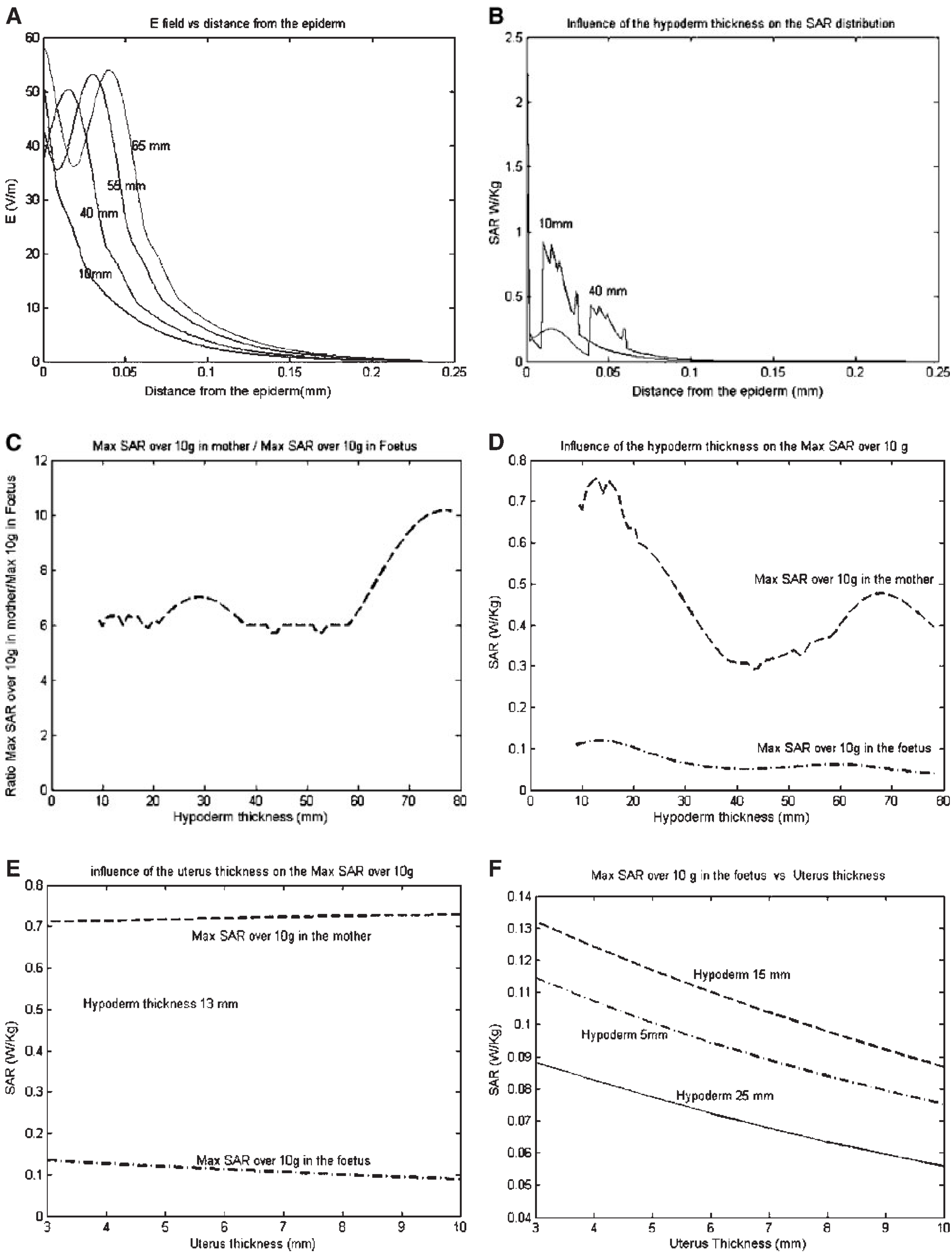

Fig. 20. E field (**A**) and SAR (**B–F**) assessment in foetus using a multilayer approach at 900 MHz.

rarely performed on fetuses. Data are sparse; although some data are available, for example, on the uterus thickness, which increases up to 3 cm at 4th month and is between 4 and 10 mm at term, we have not found data on the hypoderm thickness of pregnant woman. Since this layer could play a role of matching, we performed a parametric analysis using a planar multilayer analysis.

Based on theoretical method of plane wave propagation in layered structures, a multilayer (Fig. 19) structure composed of skin, hypoderm, muscle, uterus, placenta, amniotic fluid (considered here as cephalo spinal fluid or CSF), and fetus (considered here as muscle) was analyzed.

We considered a thickness of the skin of 2 mm, the one of muscle and uterus 5 mm, the thickness of placenta and amniotic fluid 10 mm and 2 mm, respectively. The thickness of the hypoderm is considered between 8 and 70 mm. At a frequency of 900 MHz and using relevant dielectric properties of tissues, the incident electric field (120 V/m) leads to a SAR value of 0.8 W/kg in a liquid equivalent to the head.

Figure 20 summarizes the results. With frequencies higher than 900 MHz, the ratio of Max SAR in fetus and mother seems (see Fig. 20C) to be lower than 1/6. Nevertheless since a simplified model has been used, these results have to be considered as preliminary and should be confirmed with realistic models of tissues and sources.

CONCLUSION

This study analyzes the SAR in children. The SAR estimated in the SAM is compared to the SAR estimated a child head model built using a morphing approach of visible human. The maximum SAR over 10 g in SAM has been found to be twice that in the child head. Therefore SAM can be considered as conservative to check the compliance to the related limits.

The morphology and the external head shape depend on the age. The influence of the head model on SAR in specific tissues has been investigated. Comparisons between SAR in adult heads and in children head models based on MRI have been performed and are discussed in the document.

Dealing with the maximum SAR over 10 g, the observed differences are comparable to those observed using different adult heads. It is found in the analysis of the SAR induced in brain that the max SAR over 1 g in children brain is slightly more significant than the one for the adult, while it remains at a weak level of exposure.

Using a multilayer approach, a preliminary assessment of SAR in the fetus has been investigated. With frequencies higher than 900 MHz the ratio of Max SAR in mother and fetus has been found higher than six.

Since organs are affected by large variability, the study carried out in this study has to be confirmed using extensive analysis based on a larger number of head models.

ACKNOWLEDGMENTS

This study has been carried out within the French ADONIS project (www.tsi.enst.fr/adonis/) which is supported by the RNRT network (Réseau National de Recherche en Télécommunication, www.telecom.gouv.fr/rnrt/). The authors gratefully acknowledge the advice of Dr René de Sèze from INERIS.

REFERENCES

Beard B, et al. 2003. Protocol for the computational comparison of the SAM phantom to anatomically correct models of the human head. IEEE SCC34 SC2 WG2. US Food & Drug Administration.

Berenger JP. 1994. A perfectly matched layer for the absorption of electromagnetic waves. J Comput Phys 4:185–200.

CENELEC EN50361. 2001. Basic standard for the measurement of specific absorption rate related to human exposure to electromagnetic fields from mobile phones.

Drossos A, Santomaa V, Kuster N. 2000. The dependence of electromagnetic energy absorption upon human head tissue composition in the frequency range of 300–3000 MHz. IEEE Trans Microw Theory Tech 48(11):1988–1995.

Farkas MD, et al. 1994. Antropometry of the head and face, 2nd edn. New York: Raven press.

Gabriel C. 1996. Compilation of the dielectric properties of body tissues at RF and microwave frequencies. Brooks Air Force Technical Report AL/OE-TR-1996-0037 [Online]. Available: http://www.fcc.gov/cgi-bin/dielec.sh.

Gandhi OP, Kang G. 2002. Some present problems and proposed experimental phantom for SAR compliance testing of cellular telephones at 835 and 1900 MHz. Phys Med Biol 47:1501–1518.

Gandhi OP, Lazzi G, Furse CM. 1996. Electromagnetic absorption in the human head and neck for mobile telephones at 835 MHz and 1900 MHz. IEEE Trans Microw Theory Tech 44:1884–1897.

ICNIRP guidelines. 1998. Guidelines for limiting exposure to time varying electric, magnetic, and electromagnetic field (up to 300 GHz). Health Phys 74:494–522.

IEC PT 62209 Part1. 2005. Procedure to measure the specific absorption rate (SAR) in the frequency range of 300 MHz to 3 GHz—Part 1: hand-held mobile wireless communication devices.

IEEE. 1999. Standard for safety with respect to human exposure to radiofrequency electromagnetic fields, 3kHz to 300 GHz. IEEE Standard C95.1:1999

Koenig WJ, Donovan JM, Pensler JM. 1995. Cranial bone grafting in children. Plast Reconstr Surg 95:1–4.

Schoenborn F, Burhardt M, Kuster N. 1998. Difference in energy absorption between heads of adults and children in the near field of sources. Health Phys 74(2):160–168.

Seidenari S, et al. 2000. Thickness and echogenicity of the skin in children as assessed by 20 MHz Ultrasound. Dermatology 201:218–222.

Sempé M. 1979. Auxologie, methods et sequences. Paris: Theraplix.

Taflove A. 1995. Computional electrodynamics. In: Taflove A, editor. The FDTD method. Boston, MA: Artech House.

Van Rongen E, et al. 2004. Mobile Phone. Is precautionary warranted? Bioelectromagnetism 25:142–144.

Wang J, Fujiwara O. 2003. Comparison and evaluated of electromagnetic absorption characteristics in realistic children for 900-MHz mobile telephones. IEEE Trans microw Theory Tech 51:966–971.